International Immunopharmacology 76 (2019) 105913

Contents lists available at ScienceDirect

International Immunopharmacology

journal homepage: www.elsevier.com/locate/intimp

1,4-Dithiothreitol treatment ameliorates hematopoietic and intestinal injury in irradiated mice: Potential application of a treatment for acute radiation syndrome

Kui Li, Junling Zhang, Jian Cao, Xuejiao Li, Hongqi Tian*

Tianjin Key Laboratory of Radiation Medicine and Molecular Nuclear Medicine, Institute of Radiation Medicine, Chinese Academy of Medical Science & Peking Union Medical College, Tianjin 300192, China

ARTICLE INFO

Keywords:
Ionizing radiation
1,4-Dithiothreitol
Hematopoietic progenitor/stem cells
Small intestine
P53
Radioprotection

ABSTRACT

Radiation exposure poses a significant threat to public health, which can lead to acute hematopoietic system and intestinal system injuries due to their higher radiation sensitivity. Hence, antioxidants and thiol-reducing agents could have a potential protective effect against this complication. The dithiol compound 1,4-dithiothreitol (DTT) has been used in biochemistry, peptide/protein chemistry and clinical medicine. However, the effect of DTT on ionizing radiation (IR)-induced hematopoietic injury and intestinal injury are unknown. The current investigation was designed to evaluate the effect of DTT as a safe and clinically applicable thiol-radioprotector in irradiated mice. DTT treatment improved the survival of irradiated mice and ameliorated whole body irradiation (WBI)-induced hematopoietic injury by attenuating myelosuppression and myeloid skewing, increasing self-renewal and differentiation of hematopoietic progenitor cells/hematopoietic stem cells (HPCs/HSCs). In addition, DTT treatment protected mice from abdominal irradiation (ABI)-induced changes in crypt-villus structures and function. Furthermore, treatment with DTT significantly enhanced the ABI-induced reduction in Olfm4 positive cells and offspring cells of $Lgr5^+$ stem cells, including $lysozyme^+$ Paneth cells and $Ki67^+$ cells. Moreover, IR-induced DNA strand break damage, and the expression of proapoptotic-p53, Bax, Bak protein and antiapoptotic-Bcl-2 protein were reversed in DTT treated mice, and DTT also promoted small intestine repair after radiation exposure via the p53 intrinsic apoptotic pathway. In general, these results demonstrated the potential of DTT for protection against hematopoietic injury and intestinal injury after radiation exposure, suggesting DTT as a novel effective agent for radioprotection.

1. Introduction

Ionizing radiation (IR) may have a significant impact on bone marrow hematopoietic, gastrointestinal and neurological systems [1–4]. Evidence has indicated that the hematopoietic system and small intestinal system are the major injury sites during radiation accidents and radiotherapy because of their higher radiation sensitivity [5]. The bone marrow hematopoietic system is the most sensitive to radiation among organs/tissues. Therefore, it seems extremely important to protect this system with radioprotectors for better survival and quality of life after exposure. Bone marrow damage can lead to a sharp decrease in the number of red blood cells, white blood cells and platelets, which causes hematopoietic function suppression, and hemogram changes resulting in anemia, hemorrhage and infection [6]. Notably, more serious symptoms and difficult treatments are observed after increased exposure. Generally, primary hematopoietic fatal injuries occur at doses of less than 8 Gy after WBI [7]. The recovery of the hematopoietic system depends on the proportion of surviving hematopoietic progenitor cells/ hematopoietic stem cells [HPCs/HSCs) in the bone marrow after the whole body irradiation (WBI) [7]. Additional, evidence has indicated that excess reactive oxygen species (ROS) produced by radiation could result in HSC apoptosis, senescence and loss of the capacity for self-renewal [8–10].

Acute intestinal syndrome is the main cause of death in the first

Abbreviations: IR, ionizing radiation; BM, bone marrow; WBI, whole body irradiation; ABI, abdominal irradiation; HPCs, hematopoietic progenitor cells; HSCs, hematopoietic stem cells; ROS, reaction oxygen species; DTT, 1,4-dithiothreitol; Olfm4, olfactomedin 4; ISCs, intestinal stem cells; γ-H2AX, phosphorylated histone H2AX; SSBs, single-strand breaks; DSBs, double-strand breaks; WBC, white blood cell; RBC, red blood cell; H&E, hematoxylin and eosin; PUMA, p53 upregulated modulator of apoptosis

* Corresponding author.
E-mail address: tianhongqi@irm-cams.ac.cn (H. Tian).

https://doi.org/10.1016/j.intimp.2019.105913
Received 19 June 2019; Received in revised form 29 August 2019; Accepted 12 September 2019
Available online 15 October 2019

week after exposure to high doses of radiation. The rapid and destructive injury of intestinal epithelial cells mainly induces intestinal electrolyte imbalance, poor nutrition absorption, intestinal pathogen translocation, and eventually the significant increasing risk of death resulting from the loss of intestinal function [11,12]. Mason et al. [13] showed IR-induced gut injury in a murine model after exposure to 8 Gy, with the obvious characterized responses being the apoptosis of cells within crypts of intestinal epithelium and a shortened villi compartment, followed by partial recovery. As intestinal stem cells can provide sufficient energy to small intestinal epithelial cells, the stem cells become one of the rapidly regenerated adult tissues in mammals, with a turnover rate of approximately 3–5 days in mice [5,14]. However, murine exposure to 12 Gy radiation can cause more serious damage to the intestinal epithelium, especially when intestinal stem cells cannot be reversed by any therapeutic treatment [15,16].

Generally, high-dose exposure leads to more severe symptoms, more difficult treatments, and lower survival rates. Considering the difficulty in recovery of IR-induced acute injury, it is apparently very important to search for novel radioprotectors with high efficacy. In recent years, aminothiols, natural antioxidants, hormone drugs and biological macromolecular agents, a series of compounds with the effects of radioprotection have been developed, including amifostine, cysteine, estrogens, and vitamins [16–18]. However, most of these compounds do not have clear efficacy and excellent performance. Thus far, amifostine has been the only clinical radioprotector approved by the FDA for the treatment of xerostomia with radiotherapy of head and neck cancer [19]. Nonetheless, because the effective dose of amifostine is close to the minimum toxicity dose, dose increases could lead to significant adverse effects and limit its extensive use. Compared to other types of radioprotectors, aminothiols rapidly increase the resistance of cells to radiation and resist high doses of radiation [20]. IR can lead to large numbers of radiation-by-products including $^{\cdot}OH$, $H^{\cdot}$, H_2O_2, etc., through decomposing water molecules in the cell. Many reactive oxygen species (ROS) are generated to destroy biological macromolecules and lead to organ dysfunction [21]. One of the main mechanisms of amifostine is that the metabolite (WR1065) in the presence of −SH groups can scavenge oxygen free radicals produced by ionizing radiation, thereby preventing oxygen free radicals from destroying intracellular macromolecules.

1,4-Dithiothreitol (DTT), is a dithiol compound with effective applications in biochemistry, and peptide/protein chemistry [22,23]. The main role of DTT in molecular biological assays is to keep proteins in a reduced state [24]. Thiol containing compounds have also been shown to be very effective at protecting DNA from irradiation damage [25–27], which may be due to their ability to scavenge oxygen and nitrogen radicals. The protective effect of DTT against toxic insults has been demonstrated [28,29]. However, whether DTT could ameliorate IR-induced acute hematopoietic and intestinal syndrome remains unknown.

The current investigation was designed to evaluate the effect of DTT treatment on IR-induced hematopoietic and intestinal injury. Changes in the complete blood count (CBC) of bone marrow injury, proportion of surviving HPCs/HSCs, tissue histopathological alterations, proliferation and maintenance of the regeneration of ISCs, DNA damage accumulation, and pro-apoptotic and anti-apoptotic protein alterations were monitored to evaluate whether DTT has any protective properties in irradiated mice. The data obtained from the current study might help to develop a safe and clinically applicable pharmaceutical intervention against acute radiation syndrome (ARS) and its associated complications.

2. Materials and methods

2.1. Mice

Male C57BL/6J mice aged 6–8 weeks old (20–22 g) were purchased from Beijing Huafukang Bioscience Co. Inc. (Beijing, China). All mice were maintained under specific pathogen-free conditions in the Central Animal Care Services of the Institute of Radiation Medicine, Chinese Academy of Medical Sciences, and Peking Union Medical College, People's Republic of China (IRM-PUMC, Tianjin, China). After 7 days of feeding (21–23 g), the mice were radiated. The mice were fed under a 12 h light/dark cycle during the experiment. All animal experiments were treated according to the regulations of Animal Care and Ethics Committee of IRM-PUMC (IRM-DWLL-2018062).

2.2. Reagents and antibodies

1,4-Dithiothreitol was purchased from Bide.Pharm (Shanghai China). Bradford reagent, protease inhibitor cocktail, RIPA buffer, bicinchoninic acid (BCA) protein assay kit, sodium dodecyl sulfate (SDS), formalin, ethylenediaminetetraacetic acid (EDTA), NaCl, ethanol, Tris–HCL, phosphate buffer saline (PBS), and RBC lysing buffer were purchased from solarbio (Beijing China). ECL chemiluminescence reagent was purchased from Absin (Shanghai China). Anti-mouse CD117 (c-kit) APC (clone 2B8), anti-mouse Ly-6 A/E (Sca1) PE (clone D7) and anti-mouse CD3-APC (clone145-2C11) were purchased from eBioscience (San Diego, CA, USA). PerCP streptavidin, anti-mouse CD3 APC (clone145-2C11), anti-mouse/human CD45R/B220 FITC (clone RA3-6B2), anti-mouse/human CD11b PE (clone M1/70), anti-mouse Ly-6G/Ly-6C (Gr-1) PE (clone RB6-8C5), biotin anti-mouse CD4 (clone GK1.5), biotin anti-mouse CD8 (clone 53–6.7), biotin anti-mouse/human CD45R/B220 (clone RA3-6B2), biotin anti-mouse/human CD11b (clone M1/70), and biotin anti-mouse Ly-6G/ Ly-6C(Gr1) (clone RB6-8C5) were obtained from Biolegend (San Diego, CA, USA). Anti-p53 (48818s), and anti-olfm4 (39141s) were purchased from CST (Danvers, MA, USA). Anti-lysozyme (ab108508), anti-caspase9 (ab202068), anti-caspase-3 (ab13847), anti-p53 (ab26), anti-PUMA (ab9643), anti-Bax (ab32503), anti-Bak (ab32371), anti-Bcl-2 (ab692), HRP-conjugate secondary antibody (ab7403, ab150113), anti-β-actin (ab8226) were purchased from Abcam (Cambridge, UK, USA). Anti-γH2AX was obtained from BD biosciences (NJ, USA). Anti-Ki67 antibody was purchased from Novus (Littleton, CO). The DAB kit was purchased from Sigma Aldrich (St. Louis, MO). Horseradish peroxidase secondary antibody (sc51948) was obtained from Santa Cruz Biotechnology (Santa Cruz, CA). Goat serum was purchased from Thermo Fisher Scientific (Waltham, MA).

2.3. Acute toxicity assay

An acute toxicity study was conducted according to the method described in OECD guideline 420 with minor modifications. A total of 70 mice were randomly allocated into seven groups of 10 mice each (5 females and 5 males). After overnight fasting, mice received a single intraperitoneal (i.p) dose of DTT at 100, 200, 300, 400, 500, and 600 mg/kg. The control group received the same volume of normal saline. After treatment, the mortality and clinical symptoms of toxicity were observed for several hours after infusion and every day for the next 14 days. The symptoms of toxicity to observe include hypo-activity, abdominal rigidity, convulsion, breathing difficulty, cyanosis, bleeding from any orifice, and compulsive behavior. The body weight of the mice was recorded on days 1 and 14. At the end of the study, all surviving animals were euthanized and the pathological changes were used for a microscopic necropsy examination.

2.4. Radiation injury mouse model and DTT treatment

The mice were randomly divided into 4 groups in survival and WBI studies: control, IR + Vehicle, IR + DTT (100 mg/kg), and IR + DTT (200 mg/kg). The mice were exposed to γ-ray (7.2 Gy and 4 Gy) whole body irradiation (WBI) at a dose rate of 0.99 Gy/min (Gammacell-40 ^{137}Cs irradiator, Atomic Energy of Canada Ltd.). For the ABI study, the

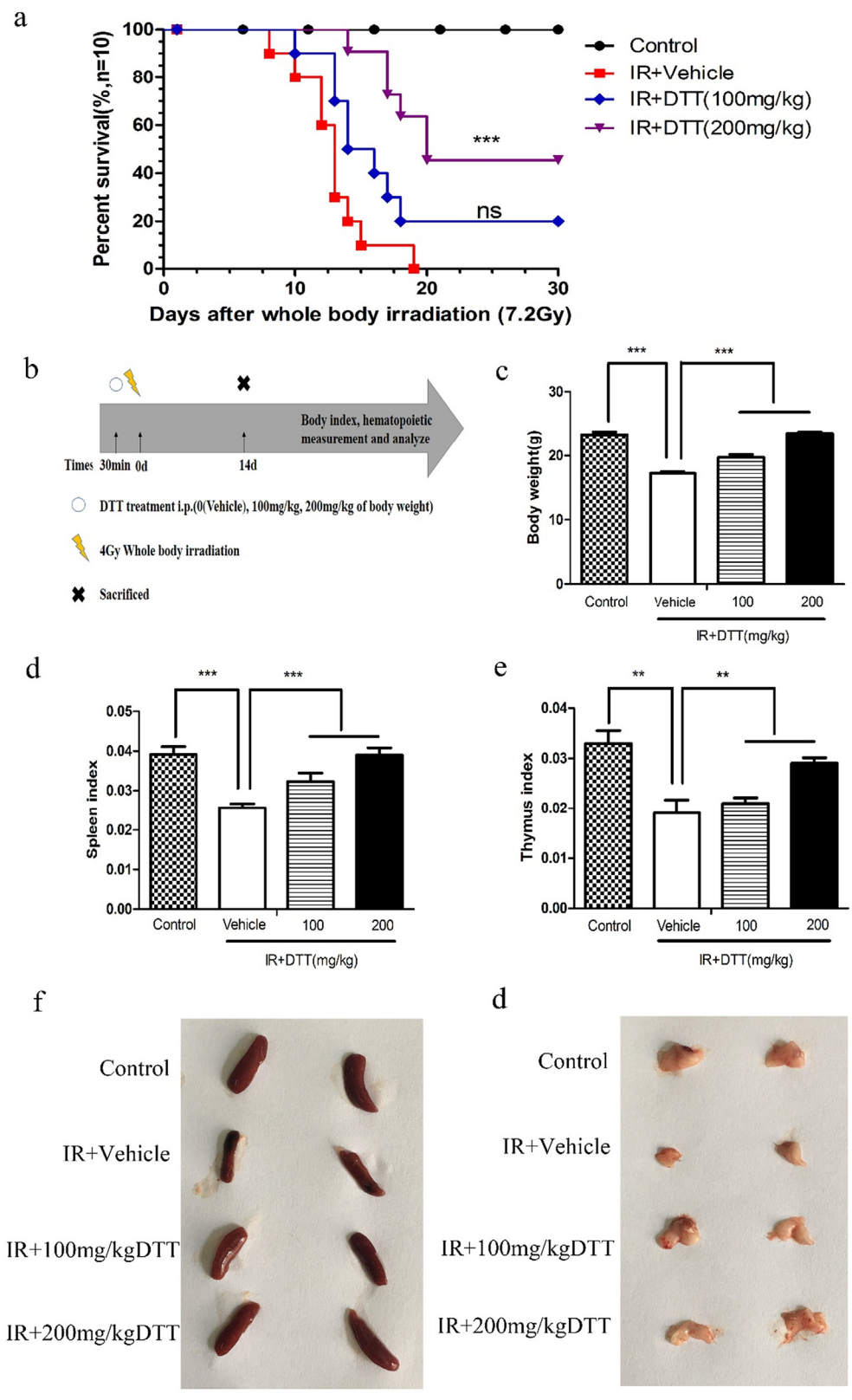

Fig. 1. DTT mitigates WBI-induced lethality and rescues the body weight loss, organ index changes after WBI in mice. (a) Kaplan-Meier survival curve depicts the 30 days survival for the protective effects of DTT. Mice were irradiated with 7.2 Gy, and DTT were administered intraperitoneal 30 min before irradiation, ***P < 0.001 by log-rank testing between WBI-exposed mice treated with DTT/Vehicle, n = 10, the experiment of mouse survival rate were performed three repetitions. (b) Radiation injury and DTT treatment scheme for mice. Mice were randomly divided into four groups and DTT were administered intraperitoneal 30 min before irradiation. Control mice were sham-irradiated. (c) Bar graph showing the average body weight of each group. Spleen index (d) and thymus index (e) were shown by Bar graph. Representative images of spleen (f) and thymus (g) were harvested and shown. Statistical significance was analyzed as the mean ± SEM (n = 5). **P < 0.01; ***P < 0.001; IR ionizing radiation.

mice were divided into 2 groups (IR + Vehicle, IR + DTT (200 mg/kg)) in survival and 3 groups in experiment: control, IR + Vehicle, IR + DTT (200 mg/kg). The mice were exposed to γ-ray (15 Gy) abdominal irradiation (ABI) at a dose rate of 0.99 Gy/min (Gammacell-40 ^{137}Cs irradiator, Atomic Energy of Canada Ltd.). Control mice were sham-irradiated. IR was delivered using a lead shielding, except for the 2.75 cm diameter roundness exposed field in mouse abdomen and the other parts of the mouse were shielded. The mice were intraperitoneally administered DTT (solvent: normal saline) for 30 min before irradiation. Control mice and irradiated mice were administered the same volume of vehicle (normal saline) at the same frequency and through the same route as DTT.

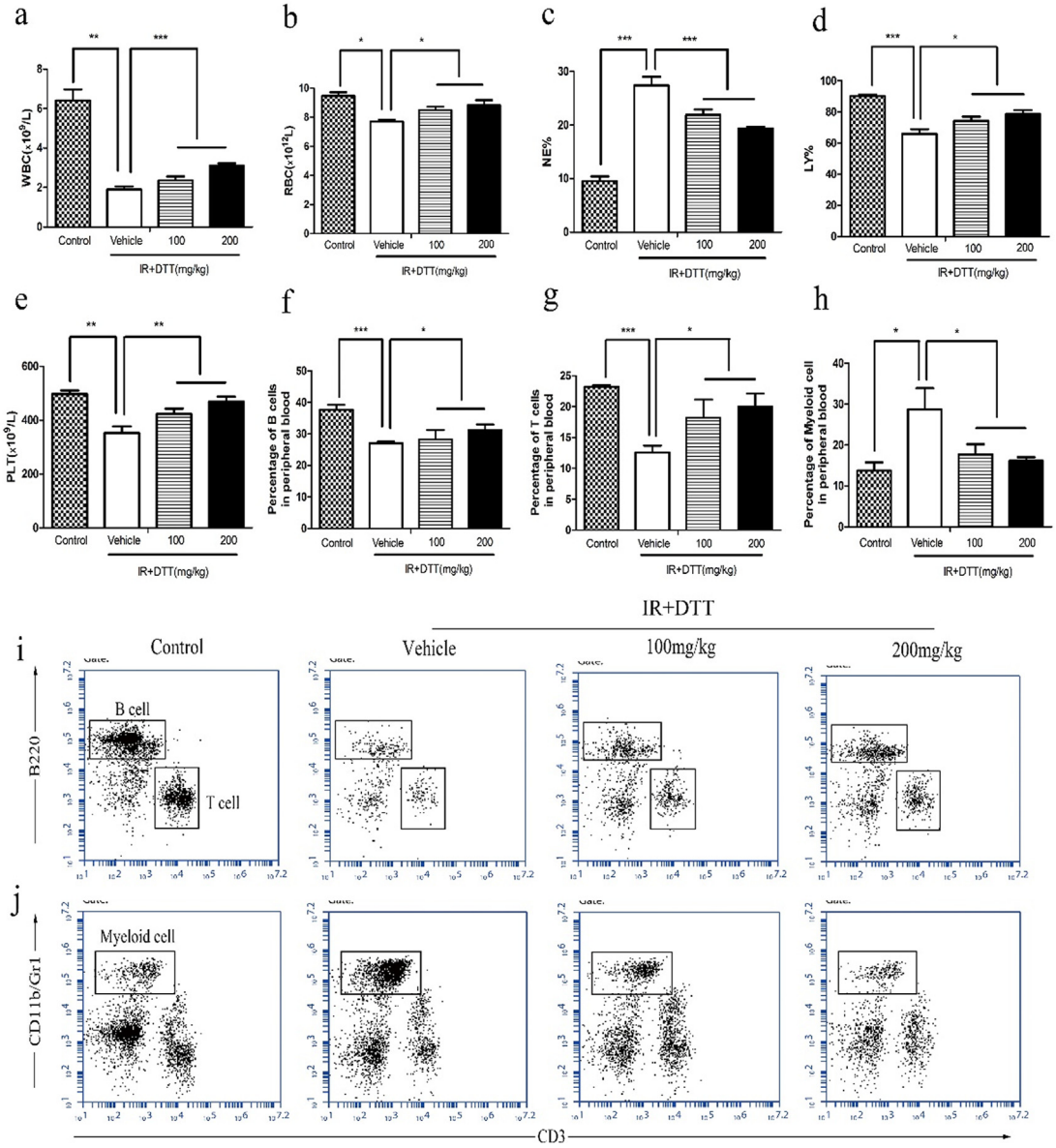

Fig. 2. DTT ameliorates WBI-induced myelosuppression and myeloid skewing. Mice were sham-irradiated as a control or irradiated with 4 Gy WBI 30 min after treated with vehicle or DTT as described in the text. (a) The number of white blood cell counts (WBC), (b) red blood cell counts (RBC), (c) percentage of neutrophil granulocytes (NE%), (d) percentage of lymphocytes (LY%) and (e) number of platelet counts (PLT) in peripheral blood were quantified 14 days after WBI. The percentage of (f) B cells, (g) T cells, and (h) myeloid cells in peripheral blood were analyzed by flow cytometry at 14 days after WBI. (i) and (j) Representative fluorescence-activated cell sorting (FACS) plots of B cells, T cells and myeloid cells. Statistical significance was analyzed as the mean ± SEM (n = 5), *P < 0.05; **P < 0.01; ***P < 0.001; IR ionizing radiation. (For interpretation of the references to color in this figure legend, the reader is referred to the web version of this article.)

2.5. Weight change, organ index, and assays for intestinal injury

For the WBI study: four groups were set as described in the radiation injury mouse model section. Body weights (g) were measured at 14 days after 4 Gy radiation. Then, the mice were euthanized, and the complete spleen and thymus were harvested and weighed to calculate the spleen index and thymus index. The organ index was calculated according to the following formula: Organ index = [organ weight (g)/body weight (g)] × 10. For the ABI study, three groups were set as described previously. The mice were sacrificed on day 5 post-irradiation to assess intestinal injury. The entire colon starting from the anus was harvested in PBS and photoed.

2.6. Peripheral blood analysis and bone marrow cell counts

Blood was directly withdrawn from the orbital sinus and collected in pre-coated K_3EDTA-containing EP tubes at 14 days following irradiation exposure from surviving mice. The blood was mixed gently on a rotary shaker and analyzed for the cell counts, including white blood cell counts (WBCs), red blood cell counts (RBCs), the percentage of neutrophil granulocytes (NE%), and the percentage of lymphocytes (LY %) and platelet counts (PLTs). Bone marrow cells were flushed out from both the tibias and femurs with sterile phosphate-buffered saline (PBS) and filtered through a 200-mesh sieve, and the cell numbers were counted using a hematology analyzer (Nihon Kohden, Japan).

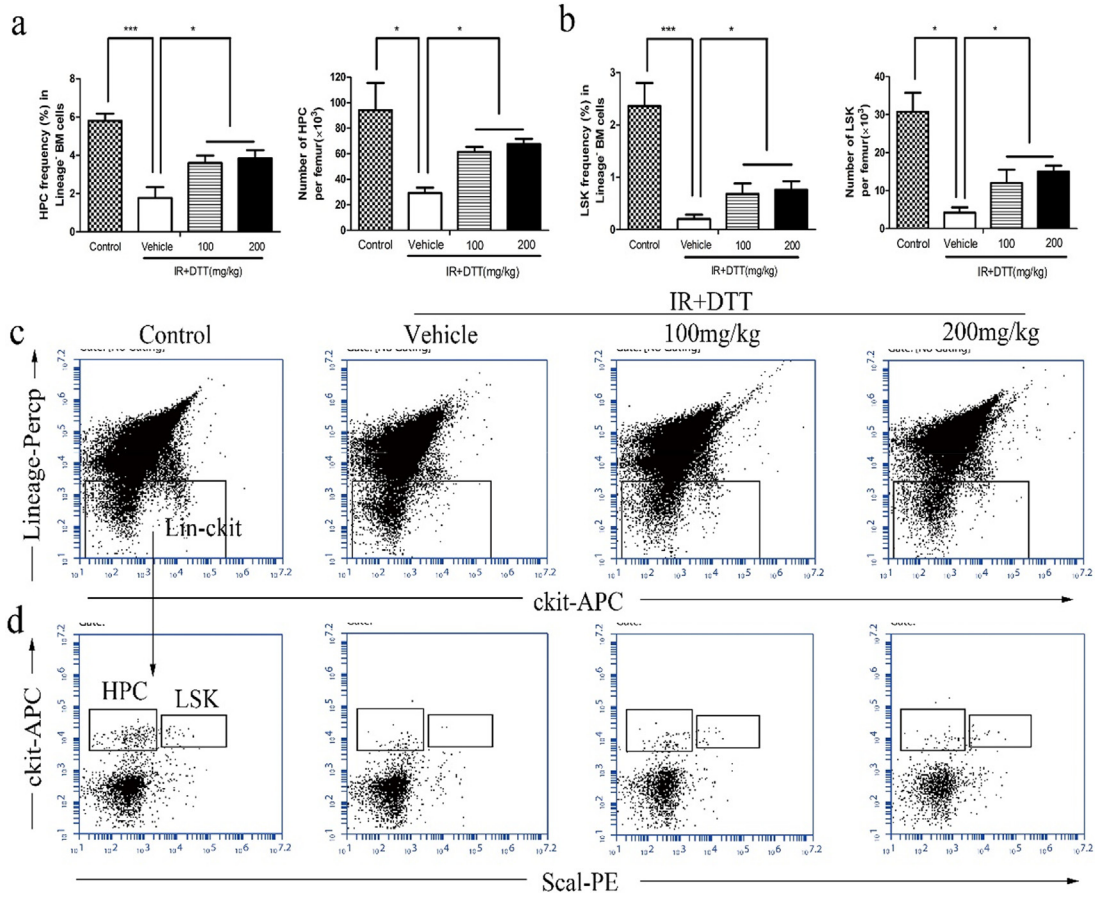

Fig. 3. DTT rescues WBI-induced decrease in bone marrow (BM) hematopoietic cells. Mice were sham-irradiated as a control or irradiated with 4 Gy WBI 30 min after treated with vehicle or DTT as described in the text. (a) Hematopoietic progenitor cells (HPCs, Lineage$^-$sca1$^-$c-kit$^+$) frequency and (b) LSKs (Lineage$^-$sca1$^+$ c-kit$^+$) frequency in Lineage$^-$ BM cells were analyzed 14 days after 4 Gy WBI. (c) and (d) Representative FACS plots show the percentage of HPCs and LSKs. Statistical significance was analyzed as the mean ± SEM (n = 5) *P < 0.05; ***P < 0.001; IR ionizing radiation.

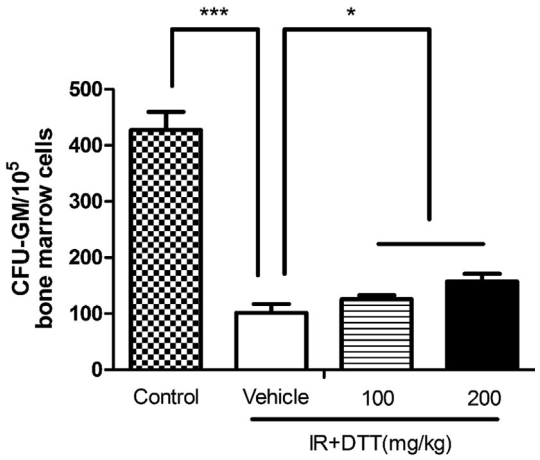

Fig. 4. DTT mitigates WBI-induced suppression of HPC function. Mice were sham-irradiated as a control or irradiated with 4 Gy WBI 30 min after treated with vehicle or DTT as described in the text. Bone marrow cells were harvest from the sacrificed mice after various treatments and cultured in M3534 methylcellulose semi-solid medium for 5 days, and then analyzed the colony-forming unit-granulocytes and macrophages (CFU-GM). The data are presented as mean ± SEM (n = 5). *P < 0.05; ***P < 0.001; IR ionizing radiation.

2.7. Flow cytometry analysis

To measure the number of B cells, T cells, and myeloid cells in peripheral blood after irradiation from surviving mice, the mice were sacrificed and peripheral blood was harvested as described previously. Fifty microliters of peripheral blood was first stained with B220, CD3, CD11b, and Gr1 antibody at room temperature, and then, the red blood cells were eliminated by the RBCs lysis buffer. For analysis of the number of HPCs and HSCs, the isolated bone marrow cells were filtered and counted as described above prior to staining with the antibodies. A total of 5×10^6 bone marrow cells were stained with biotin-labeled Ter119, B220, Gr1, CD11b, CD4, and CD8 and then stained with streptavidin, c-kit, and sca1 antibody. Data acquisition was performed on a BD Accuri C6 flow cytometer (BD Bioscience, San Jose, CA, USA) and processed using the BD Accuri C6 software.

2.8. Colony-forming cell (CFC) assay

The CFC assays were conducted by culturing bone marrow cells in M3534 methylcellulose semisolid medium (Stem Cell Technologies, Vancouver, BC, Canada). The colony forming unit-granulocyte macrophages (CFU-GM) with more than 30 cells were counted according to the manufacturer's instructions. The results are expressed as the numbers of CFU-GM per 10^5 bone marrow cells.

2.9. Tissue harvest and histological analysis

On day 5 post-irradiation, the mice were sacrificed and the small intestines were harvested and flushed with saline. The harvested intestinal tissues were divided into segments and immediately fixed in 4% neutral-buffered formalin for histological analysis. After formalin fixed tissues were embedded in paraffin, paraffin-embedded sections were

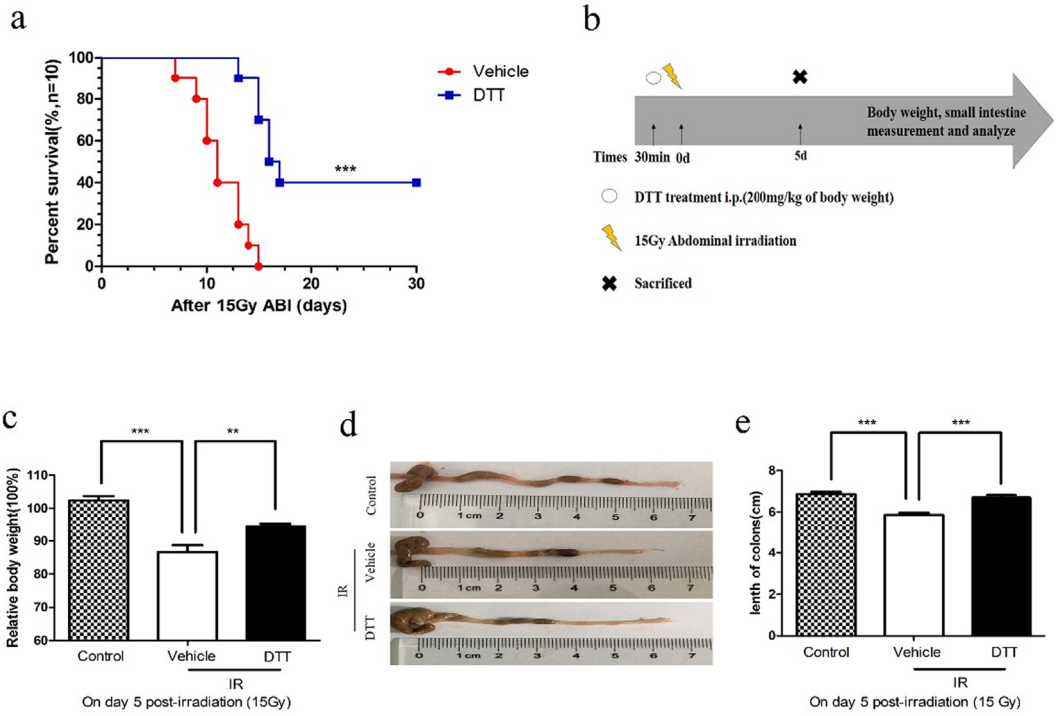

Fig. 5. DTT protects against ABI-induced lethal intestinal injury. (a) Kaplan-Meier survival curve depicts the 30 days survival for the protective effects of DTT. Mice were irradiated with 15 Gy, and DTT were administered intraperitoneal 30 min before irradiation, ***P < 0.001 by log-rank testing between ABI-exposed mice treated with DTT/Vehicle, n = 10, the experiment of mouse survival rate were performed three repetitions. (b) Schematics of DTT and radiation doses. Mice were randomly divided into three groups and DTT were administered intraperitoneal 30 min before 15 Gy ABI (abdominal irradiation). Control mice were sham-irradiated. (c) Relative BW (body weight) on days 5 after ABI compared with BW on day 0. (d) Representative pictures of colon were presented, and (e) rescued length of colons (n = 5) were treatment with DTT (200 mg/kg) in irradiated mice. Statistical significance was analyzed as the mean ± SEM (n = 5). **P < 0.01; ***P < 0.001; IR ionizing radiation.

cut into 4 μm sections stained with hematoxylin and eosin staining (H&E) and analyzed under a microscope (Olympus America, Melville, NY, USA). For morphological analysis, intestinal circular transverse sections were analyzed per mouse in a blinded manner from coded digital, H&E-stained photographs to measure the villi length, number of crypts per circumference, and the basal lamina length by using ImageJ 1.37 software.

2.10. Immunohistochemistry analysis

Sections of paraffin-embedded small intestine were deparaffinized, rehydrated, and treated with 3% hydrogen peroxide. Antigen retrieval was performed standard procedures by boiling the sections in 10 mM/L citrate buffer antigen retrieval solution (pH 9.0). Non-specific antibody binding sites were blocked by incubation with serum for 1 h at room temperature. Then, the sections were incubated with anti-Ki67 antibody (1:300 dilution), anti-olfm4 antibody (1:400 dilution), and anti-lysozyme (1:800 dilution) overnight at 4 °C, followed by incubation with horseradish peroxidase secondary antibody at a 1:200 dilution at 37 °C for 1 h. The positive cells examined by color development for signals were carried out with a DAB kit and counterstained with hematoxylin. The images were captured, analyzed, and representative positive staining images were taken using a microscope (Olympus America, Melville, NY, USA).

2.11. Immunofluorescent staining.

The paraffin-embedded sections of the small intestine were deparaffinized, rehydrated, and treated with 3% hydrogen peroxide for antigen retrieval as described and then washed thoroughly with PBS. The sections were blocked with 5% goat serum for 30 min at room temperature and then incubated with anti-γH2AX (1:1000 dilution), anti-caspase-9 (1:500 dilution), anti-caspase-3 (1:500 dilution) or anti-p53 (1:1000 dilution) overnight at 4 °C. After washing with PBS, the sections were incubated with secondary antibody at 37 °C for 1 h in darkness. Finally, the sections were sealed with 4′,6-diamidino-2-phenylindole-containing sealing agent. The images were captured by laser scanning confocal microscopy.

2.12. Protein extraction and Western blotting from intestinal tissue

On day 5 post-irradiation, the small intestines were harvested through cervical dislocation and flushed with saline. Small intestine homogenates were prepared in cold RIPA buffer containing protease inhibitor cocktail by tissue homogenizer. The homogenates were centrifuged at 10,000 RPM for 15 min at 4 °C, and the supernatants were separated without disturbing the pellet. Protein concentration was measured in supernatant and quantified using the bicinchoninic acid (BCA) protein assay kit, which was performed according to standard procedures. Equal amounts of proteins were separated using 10% SDS-PAGE. Following transfer onto nylon membrane (Merck Millipore Ltd) for 1 h, the membranes were blocked with TBST buffer (0.2 M Tris–base, 1.5 M NaCl, 0.1% Tween 20) containing 5% skimmed milk for 1 h on a shaker at room temperature. Subsequently, the membranes were incubated with the primary antibodies PUMA (1:1000 dilution), p53 (1:1000 dilution), Bax (1:1000 dilution), Bak (1:1000 dilution), Bcl-2 (1:500 dilution) and β-actin (1:1000 dilution) overnight on shaker at 4 °C. After washing twice with TBST buffer, membranes were incubated with suitable HRP-conjugated secondary antibody for 1 h at room temperature on a shaker. The membranes were again washed twice with TBST buffer and bands visualized using ECL chemiluminescence reagents. The intensities of each protein band were measured

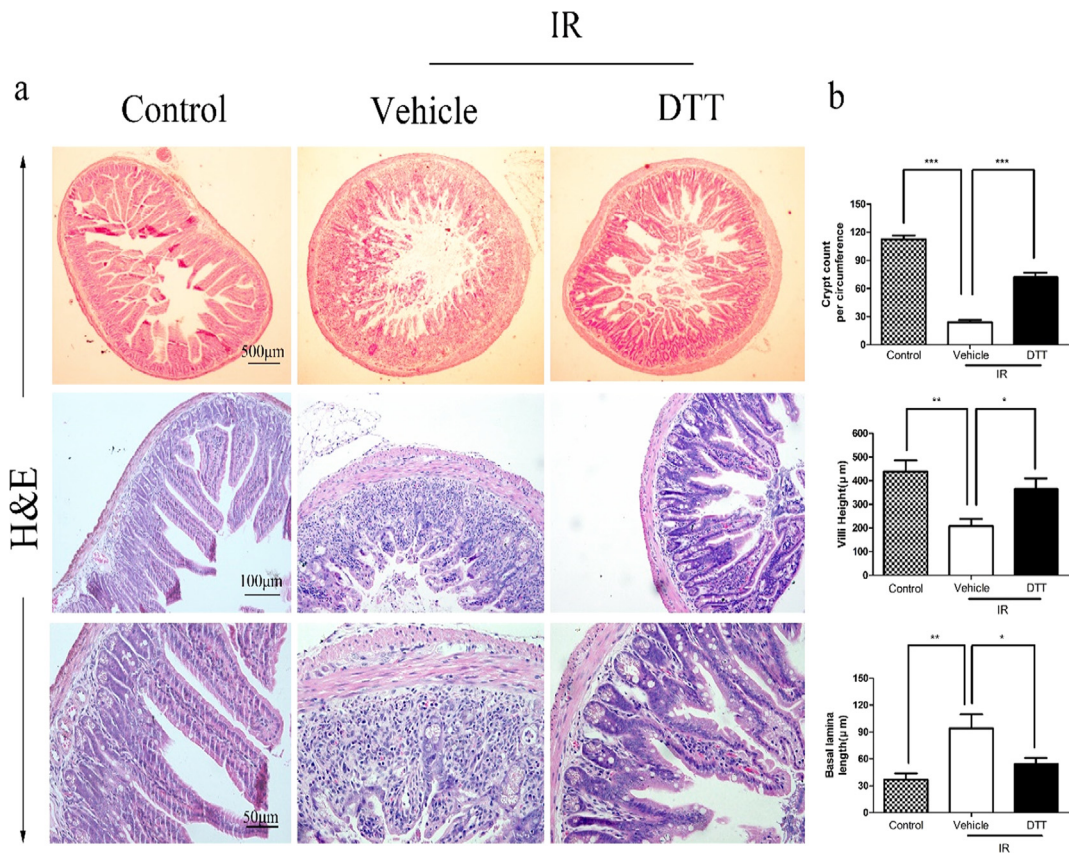

Fig. 6. Effects of DTT treatment on histologic parameters of intestinal after ABI. Mice were sham-irradiated as a control or irradiated with 15 Gy ABI 30 min after treated with vehicle or DTT as described in the text. (a) Representative hematoxylin and eosin-stained sections of mouse small intestine at days 5 post-irradiation. (b) Quantification of crypt counts per circumference, villi height, and basal lamina length for panel (a). Statistical significance was analyzed as the mean ± SEM (n = 5), *P < 0.05; **P < 0.01; ***P < 0.001; IR ionizing radiation. First row, scale bar: 500 μm; second row, scale bar: 100 μm; third row, scale bar: 50 μm.

using Image Lab™ software (Bio-Rad, USA).

2.13. Statistical analysis

All resulting data are presented as the means ± SEM. The survival curve were analyzed using the Kaplan-Meier method and Log rank test. Significant differences between experimental groups were assessed by one-way analysis of variance (ANOVA). Differences were considered significant at $p < 0.05$. All analyses were performed using GraphPad Prism 5 from GraphPad Software (San Diego, CA, USA).

3. Result

3.1. Acute toxicity of DTT by intraperitoneal injection

During the acute toxicity test, there were no deaths or any signs of toxicity observed after administration of DTT at 200 mg/kg, which was the no observed adverse effect level (NOAEL). The dose of 600 mg/kg led to the death of one female mouse within 24 h. Therefore, the median lethal dose (LD50) of DTT was estimated to be more than 600 mg/kg. Hypo-activity was observed in one male mouse at a dose of 300 mg/kg after i.p administration. Additionally, one male mouse in the 600 mg/kg group showed abdominal rigidity. The body weight gain showed no significant difference between the control and treated groups. The macroscopic observation showed no remarkable pathological changes for the tested organs.

3.2. DTT improves the survival rate of mice from a lethal dose of WBI

To ascertain whether DTT improves the survival of mice exposed to WBI, C57BL/6 mice were irradiated with 7.2 Gy and were administered DTT as described in the Material and Methods (Fig. 1b). The mouse survival rate was monitored for 30 days. As shown in Fig. 1a, none of the vehicle group mice survived for 17 days after 7.2 Gy WBI. However, compared to the vehicle group, the 100 mg/kg DTT treatment had a 20% survival rate, and the 200 mg/kg DTT treatment had a 50% survival rate. These results suggested that DTT treatment significantly increased the survival rate following a lethal dose of WBI.

3.3. DTT rescues the loss of body weight and ameliorates WBI-induced changes in spleen and thymus index

In this experiment, we observed the body weight of mice and whether DTT treatment protected mice from WBI-induced organ index changes in each group. The treatment schedule is shown in Fig. 1b. Compared to the control group, the body weight of the vehicle group decreased significantly when the mice were sacrificed at 14 days after 4 Gy WBI. However, the body weight of the mice that received 100 mg/kg and 200 mg/kg DTT was significantly increased compared to that of the vehicle group (Fig. 1c). The spleen and thymus index to some extent reflect the severity of irradiation injury and the rescue of the general condition. As shown in Fig. 1d and e, compared to the vehicle group, treatment with 200 mg/kg DTT significantly attenuated the reduction in the spleen index and thymus index after 4 Gy irradiated mice, while the 100 mg/kg DTT treatment showed a slight effect of rescues. In addition, the phenomenon of thymus and spleen atrophy in DTT treated mice was inhibited compared to that in the vehicle group (Fig. 1f and g). Our results suggested that DTT plays a protective role in WBI-induced organ injury in mice, and 200 mg/kg DTT treatment exhibits higher radioprotective efficiency than the 100 mg/kg DTT treatment.

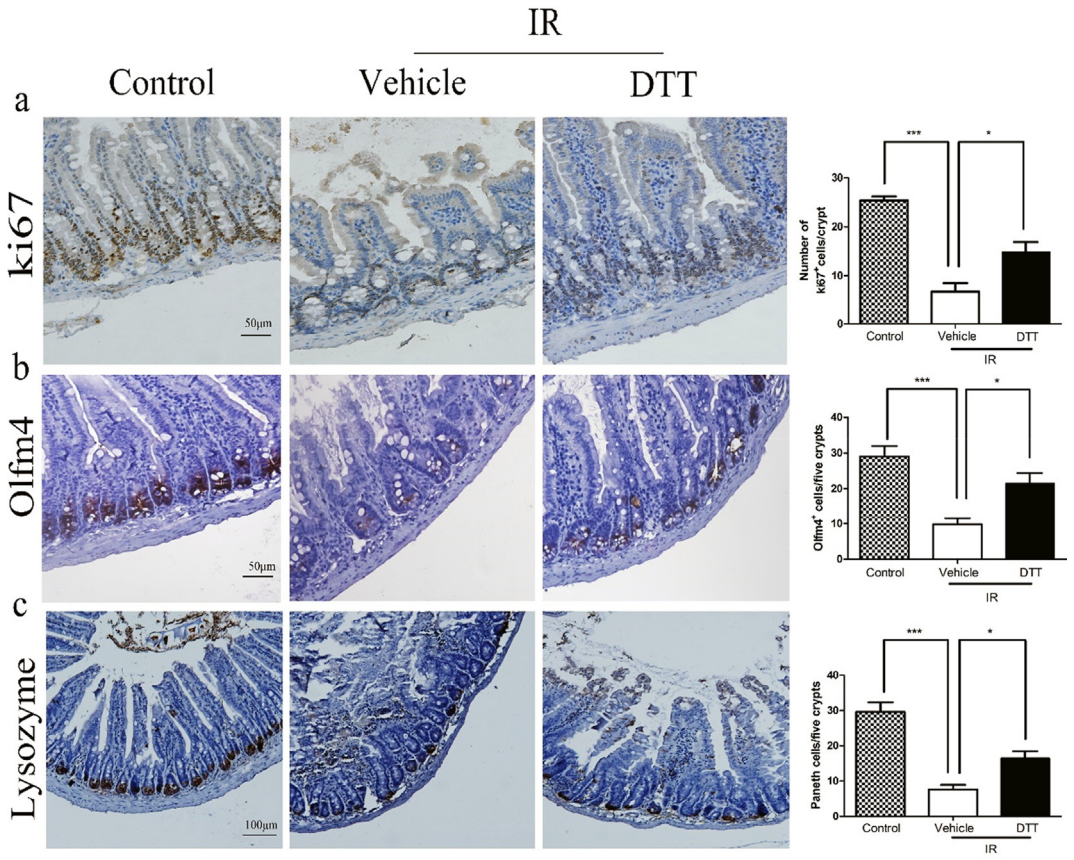

Fig. 7. DTT enhances the ISC survival and maintains the regeneration capacity of ISCs after ABI. Mice were sham-irradiated as a control or irradiated with 15 Gy ABI 30 min after treated with vehicle or DTT as described in the text. (a) Representative Ki67 immunostained intestinal sections from untreated or DTT treatment mice at days 5 post-irradiation (Scale bars: 50 μm). Bar graph showing the quantification the number of Ki67-positive cells per crypt determined from panel (a). (b) Representative images of intestinal Olfm4 positive cells from untreated or DTT treatment mice at days 5 post-irradiation (Scale bars: 50 μm). Bar graph showing the quantification the number of the intestinal Olfm4 positive stem cells determined from panel (b). (c) Representative immunohistochemistry images for lysozyme stained sections of small intestine from untreated or DTT treatment mice at days 5 post-irradiation (Scale bars: 100 μm) and Bar graph showing the quantification the number of Paneth cells/five crypts unit determined from panel (c). Statistical significance was analyzed as mean ± SEM, (n = 5). *P < 0.05; ***P < 0.001; IR ionizing radiation.

3.4. DTT alleviates myelosuppression and promotes myeloid skewing recovery in vivo

WBI-induced myelosuppression has been established, which is manifested as decreased bone marrow activity, resulting in a significant decline of peripheral blood cells [30]. The decrease of lymphoid cells and increase of myeloid cells has been identified as a remarkable symptom of IR-induced impaired differentiation of hematopoietic stem cells (HSCs). HSCs must be differentiated into different blood cell lineages and balanced to prevent lineage skewing [6,10] To investigate the protective effects of DTT on the hematopoietic system against ir-radiation, we examined the abundance of different types of hemato-poietic cells in peripheral blood cell counts using an automatic blood-counter system and flow cytometry. As shown in Fig. 2, compared with the control group, the mice receiving 4 Gy WBI exhibited a substantial decrease in white blood cells (WBCs), red blood cells (RBCs), platelet levels (PLT) and percentage of lymphocyte cells (LY%) including T cells and B cells, and the percentage of neutrophils (NE%) and myeloid cells increased significantly in these mice. Treatment with 200 mg/kg DTT significantly reversed the changes in peripheral blood cells in irradiated mice. The results suggest that DTT treatment improves its recovery from WBI induced myelosuppression and myeloid skewing and main-tains hematopoietic homeostasis.

3.5. DTT rescues the decrease in mouse bone marrow hematopoietic cells after WBI

Radiation induces bone marrow (BM) hematopoietic cell damage and affects all lineages of blood cells. Protecting and rescuing hema-topoietic cells from radiation damage is important in the treatment of radiation injury [10,31]. Therefore, we investigated the effects of DTT treatment on hematopoietic cells. The bone marrow hematopoietic cell population at 14 days after 4 Gy WBI was analyzed. We measured the percentage of bone marrow LSK cells (Lin^- $Sca\text{-}1^+$ $c\text{-}kit^+$) and HPC cells (Lin^- $Sca\text{-}1^-$ $c\text{-}kit^+$) using flow cytometry. As shown in Fig. 3, compared with the control group, the vehicle group exhibited a de-crease in the frequency of LSKs and HPCs. However, two doses of DTT increased the number of LSKs and HPCs in mice after 4 Gy WBI, and 200 mg/kg DTT treatment performed better. These findings indicated that DTT alleviates the WBI-induced dysfunction of LSKs and HPCs.

3.6. DTT mitigates WBI-induced suppression of HPC function

In addition, we performed a CFC assay to examine whether hema-topoietic cells from irradiated mice maintained their clonogenic func-tion after DTT treatment. As shown in Fig. 4, WBI caused a considerable suppression of HPC clonogenic function, whereas mice that received DTT treatment after exposure to 4 Gy WBI showed the dramatically increased the production of CFU-GM. These results suggest that DTT could attenuate the WBI-induced suppression of hematopoietic

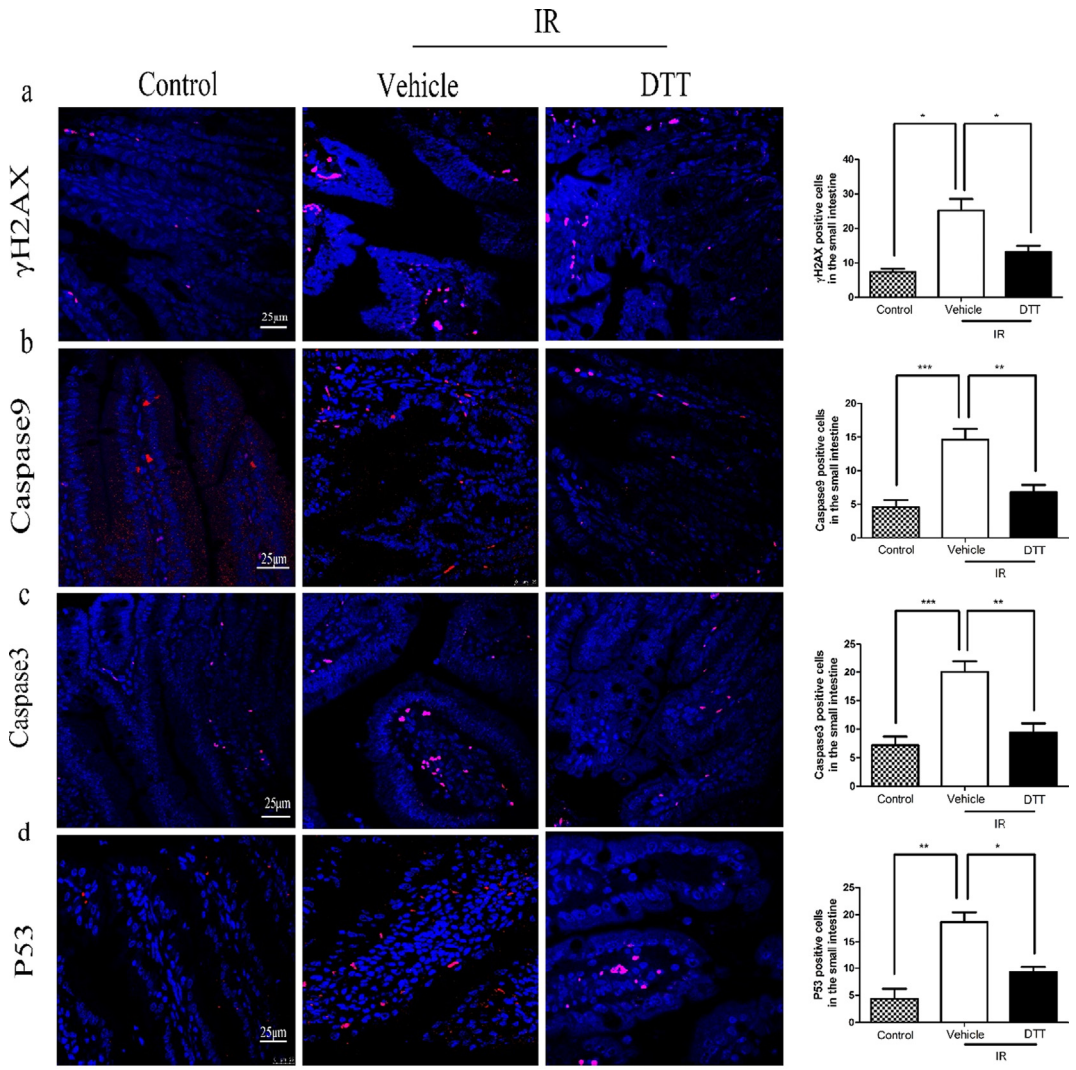

Fig. 8. DTT attenuates ABI-induced DNA damage accumulation, curtailed ABI-induced apoptosis and downregulated p53 expression in the small intestine. Mice were sham-irradiated as a control or irradiated with 15 Gy ABI 30 min after treated with vehicle or DTT as described in the text. (a) Representative confocal images of γH2AX (red) staining in the crypts from untreated or DTT treatment mice, Blue: DAPI. (Scale bars: 25 μm). Bar graph shows the quantification of γH2AX foci in intestinal epithelia cells. (b) Representative confocal images of caspase9 staining (red) of intestinal epithelia cells from untreated or DTT treatment mice, Blue: DAPI. (Scale bars: 25 μm). Bar graph shows the quantification of caspase9 foci in intestinal epithelia cells. (c) Representative confocal images of caspase3 staining (red) of intestinal epithelia cells from untreated or DTT treatment mice, Blue: DAPI. (Scale bars: 25 μm). Bar graph shows the quantification of caspase3 foci in intestinal epithelia cells. (d) Representative confocal images of p53 staining (red) of intestinal epithelia cells from untreated or DTT treatment mice, Blue: DAPI. (Scale bars: 25 μm). Bar graph shows the quantification of p53 foci in intestinal epithelia cells. Statistical significance was analyzed as mean ± SEM, (n = 5 in a, b and c, n = 3 in d). *P < 0.05, **P < 0.01; ***P < 0.001; IR ionizing radiation. (For interpretation of the references to color in this figure legend, the reader is referred to the web version of this article.)

progenitor cells.

3.7. DTT potently protects against ABI-induced lethal intestinal injury

To determine the role of DTT on IR-induced lethal small intestinal injury in irradiated mice, we first investigated the survival of mice after 15 Gy ABI with DTT treatment at 30 min before radiation exposure. As shown in Fig. 5a, we observed that all the mice in the vehicle control group died, while the mice survival rate was 40% after exposure to 15 Gy ABI. Moreover, compared to the control group, vehicle-treated mice had an average weight loss of 13.3 ± 4.5% at 5 days after ABI (Fig. 5c), which is characteristic of lethal intestinal injury [32]. In contrast, only an average weight loss of 5.4 ± 1.8% was observed in the DTT treatment group. In addition, the colons of the mouse in the vehicle group were shortened compared with those of the mice in the control group after ABI; however, treatment with 200 mg/kg DTT notably rescued the length of the colons in mice (Fig. 5d and e). These results demonstrated that DTT could protects against ABI-induced lethal intestinal injury.

3.8. DTT reduces the damage to intestinal morphology in mice after ABI

Ionizing irradiation mediated toxicity was frequently defined as clonogenic cell death and apoptosis in the crypt cells, resulting in insufficient replacement of the villus epithelium in structure destruction, lengthening the basal lamina barrier and breakdown of the mucosal barrier leading to infiltration of inflammation [33,34]. To determine the effects of DTT on IR-induced intestinal injuries, we examined the histologic characteristics of small intestines at 5 days after ABI, as shown in Fig. 6. In contrast to the tissue sections of the intestine from the control group, the vehicle group showed the massive infiltration of inflammatory cells, the destruction of the crypt/villi structure, and a lengthened basal lamina (Fig. 6a). However, 200 mg/kg DTT treatment showed a decrease in the destroyed crypt/villi structure, protecting the

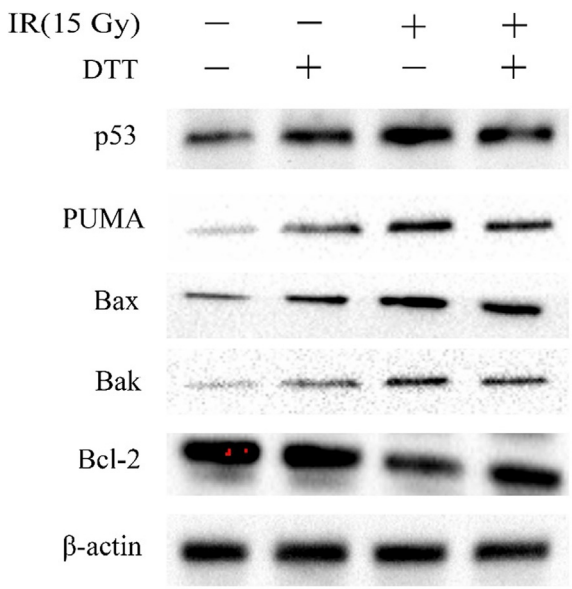

Fig. 9. Effect of DTT on modifications of intestinal apoptotic versus anti-apoptotic proteins expression pattern in mice exposed to 15 Gy WBI. The differences in expression of p53, Bcl-2 and Bax were analyzed by western blot as described in "Material and methods".

original state of basal lamina accompanied by an attenuated inflammatory response with levels compared to that of the control group. Quantitative analyses of histologic parameters (Fig. 6b) showed that vehicle groups had decreased average crypt counts per circumference (20.3 vs. 109.0), average shorter villi heights (207.5 vs. 439.0 μm), and average longer basal lamina (94.1 vs. 36.9 μm), compared to those of the control group. However, treatment with 200 mg/kg DTT showed largely rescue effects on crypt counts [66], villi height (364.6 μm) and basal lamina length (54.3 μm). These results indicated that DTT reduces the post-radiation damage of intestinal villus-crypt structures in mice.

3.9. DTT enhances the Lgr5$^+$ ISC survival and maintains the regeneration capacity of ISCs after ABI

Olfm4 protein, a robust marker of Lgr5$^+$ stem cells, has been localized to mitochondria, nuclei and cell membranes. Several studies have indicated that Lgr5 positivity at or near the crypt base indicates putative intestinal stem cells (ISCs) [35], and this marker plays an important role in intestinal regeneration following irradiation [36]. Paneth cells are specialized intestinal epithelial cells that secrete abundant antimicrobial proteins, including lysozyme. Some reports have indicated that disrupting Paneth cell secretion could lead to inflammatory disease [37–39]. In this study, we evaluated intestinal homeostasis, which was the proportion and functional integrity of proliferating crypts in the small intestines. The fraction of proliferating crypts was determined by analyzing Ki-67 immunohistochemical staining. Compared to the control group, the Ki-67 positive cells notably decreased in the vehicle group with 15 Gy ABI; however, 200 mg/kg DTT treatment significantly increased the Ki-67-positive cells within the crypt structures (Fig. 7a). Therefore, the improved intestinal tissue integrity in the DTT treatment group following irradiation may be due to the increased functionality of crypt stem cells. Then, we examined the effects of DTT on ISCs after 15 Gy ABI by Olfm4 immunohistochemical staining. Irradiation induced a greater loss of

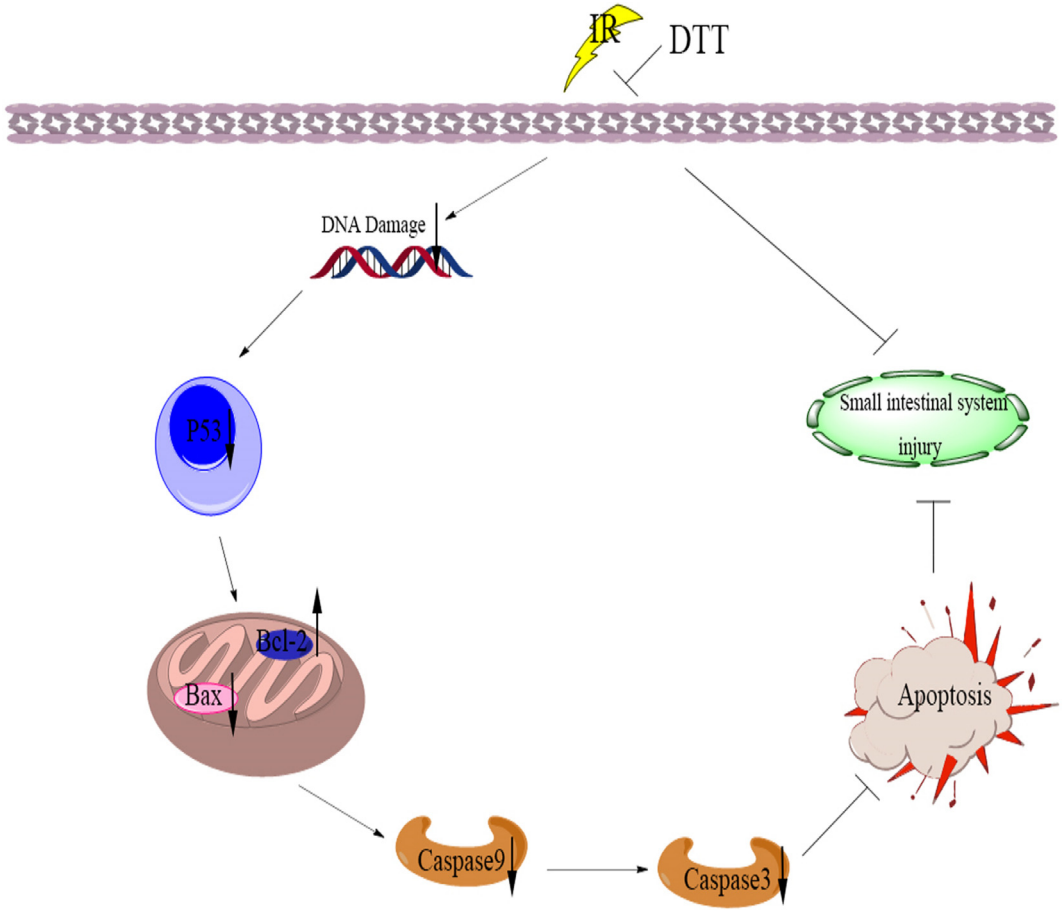

Fig. 10. A summary on the radioprotective mechanism of DTT.

Olfm4-positive cells in the vehicle group at 5 days, which was significantly reversed in the 200 mg/kg DTT treatment (Fig. 7b). In addition, we also examined the secretion of lysozyme in intestinal epithelial cells after ABI. The expression of lysozyme with a large loss in the vehicle group compared to the control group. Inversely, treatment with 200 mg/kg DTT was very potent, increasing the expression of lysozyme in crypts (Fig. 7c). Taken together, the data demonstrate that DTT treatment maintains the regenerative ability of the ISCs.

3.10. DTT attenuates DNA damage accumulation in the small intestine after ABI

Phosphorylated histone H2AX (γ-H2AX), a central player in the DNA damage response, serves as a biomarker of DNA double-stranded breaks (DSBs). Therefore, to examine the potential role of DTT treatment in ABI-induced DNA damage and repair, we detected DNA DSBs by γ-H2AX immunofluorescent staining. In the vehicle-treated group, robust γ-H2AX expression increased nearly 4 fold at 5 days after ABI compared to the control group (Fig. 8a). Treatment with 200 mg/kg DTT significantly reversed the γ-H2AX increased expression and attenuated IR-induced DNA damage, approximately reaching the same level as that of the control group at 5 days. These data demonstrated that DTT attenuates DNA damage accumulation in the small intestine after irradiation.

3.11. DTT downregulated p53 expression and alleviated ABI-induced apoptosis

P53 is the main mediator of the cell response to DNA damage by involving mechanisms that contribute to cell-cycle arrest or death in epithelial tissues. P53 and its downstream targets are closely related to cell apoptosis. Accordingly, we explored the role of DTT on ABI-induced epithelial cell apoptosis by immunofluorescent staining. In the vehicle group, irradiation significantly promoted the expression of caspase-9 (Fig. 8b), caspase-3 (Fig. 8c) and p53 (Fig. 8d) in intestinal cells. With 200 mg/kg DTT treatment, the expression of p53, caspase-3 and caspase-9 in intestinal cells decreased dramatically compared with that in the vehicle group. These results indicated that DTT profoundly suppressed radiation-induced p53 activation and apoptosis, and influenced the stress responses in the small intestine.

3.12. Effect of DTT treatment on differential pro-apoptotic and anti-apoptotic protein expression in intestinal after irradiation

Understanding the molecular mechanism is important and necessary to develop radioprotection drugs. In this study, to elucidate the protective mechanism of DTT treatment on IR-induced small intestine tissue injury, we detected the differential expression of the apoptosis proteins p53, Bak, Bax and the anti-apoptotic protein Bcl-2 in the small intestine after 15 Gy by Western blotting (Fig. 9). The level of p53 expression was significantly upregulated in 15 Gy irradiated mice compared with the control group in intestinal cells. Simultaneously, Bax expression was also upregulated in irradiated mice. However, treatment with 200 mg/kg DTT significantly inhibited the expression of p53, Bax and Bak proteins compared to that in only irradiated mice. In addition, we also assessed the expression of the anti-apoptotic protein Bcl-2. Compared with 15 Gy irradiation mice, DTT treatment increased Bcl-2 expression in intestinal cells. This result suggested that DTT treatment could reduce IR-induced apoptosis in the small intestine by regulating the intrinsic apoptotic pathway.

4. Discussion

In recent years, the incidence of malignant tumors has been on a continuous upward trend. Radiation therapy plays an indispensable role as one of the main treatments on the majority of tumors, but high-dose radiation exposure could lead to damage in normal tissues and organs around the tumor inevitable. Acute radiation syndrome caused by irradiation severely limits the wide application of radiotherapy in tumor treatment, and significantly affects the efficacy and quality of life after treatment for cancer patients. In addition, accidental radiation exposure or a terrorist attack with a radioactive dirty bomb poses a serious threat to public health [40,41]. Between 1945 and 1987, there were 285 nuclear reactor accidents, injuring 1550 people and killing 64 [2,42–44]. The most serious nuclear disaster in human history occurred in the nuclear complex of Chernobyl on 26 April 1986. Both the quantities of radionuclides released into the atmosphere induced irreversible injury to humanity health. A recent study showed that 237 individuals were involved in the early response phase and were exposed to radiation in doses high enough to cause tissue reactions, among whom 134 individuals were further diagnosed with acute radiation syndrome (ARS) and 30 patients died shortly after the accident [45]. These nuclear and radiological emergencies require comprehensive medical preparedness and readiness, including a national stockpile of deliverable agents to counteract radiation exposure incidents and accidents.

In the past few years, researchers have designed and synthesized a variety of radioprotectors to provide protection against the effects of ionizing radiation in mammals and living organisms, including thiol compounds, hormones, cytokines, etc. [17,46]. Compared to other types of radioprotectors, thiol compounds have the unique advantage of rapidly increasing the resistance of cells to ionizing radiation in the presence of both the −SH and $-NH_2$ groups [20]. However, the potential of DTT as a radiation protectant and mitigate acute radiation syndrome has not been investigated. In our pre-liminary experiment, according to the acute toxicity reaction study, the highest dose of DTT that could be administered was 200 mg/kg. Under our experimental conditions, we found that treatment with 200 mg/kg DTT exhibited a greater radioprotective effect than treatment with 100 mg/kg DTT. These data suggested that DTT at low-doses was unable to efficiently protect mice against IR-induced injury.

Bone marrow is the primary hematopoietic tissue, and the extent of hematopoietic function damage is positively correlated with the level of irradiation dose. Moreover, anemia caused by the decrease in mature RBCs, bleeding resulting from decreased PLTs, and infection due to WBCs decrease exerts a serious impact on the survival of animals after radiation exposure. The above pathological changes are mainly due to the suppression of hematopoiesis dominated by apoptosis of hematopoietic cells in the bone marrow. Therefore, reducing the suppression of hematopoiesis may alleviate injury in irradiated animals [10]. Davis TA and coauthors [47] reported that WBCs, RBCs and PLTs are both sensitive in peripheral hemograms to ionizing irradiation. Our study showed that the peripheral blood WBC, RBC and PLT counts dropped remarkably in irradiated mice at 14 days after WBI. This finding is consistent with previous studies. However, the peripheral hemogram of mice in the 200 mg/kg DTT treatment significantly rescued the decreases in WBC, RBC and PLT counts 14 days after injury. In addition, Wang et al. demonstrated that lymphoid-biased HSCs performed more sensitive to irradiation-induced differentiation, compared to myeloid-biased HSCs, leading to an imbalance in myeloid and lymphoid differentiation in irradiated mice [6], manifested as the reduced proportion of B cells and T cells, and the increased proportion of myeloid cells. The flow cytometry results revealed that 200 mg/kg DTT treatment 30 min before irradiation substantially reduced myeloid skewing induced by irradiation with 4 Gy. Previous studies have demonstrated that sub-lethal doses of irradiation (such as 4.0 Gy, 6.0 Gy WBI) resulted in long-term residual injury in the hematopoietic system via reduced HSC reserves and defective HSC function [8,48–50]. Furthermore, a number of HSCs may have the ability to repair radiation-induced damage or are spared from damage and are able to repopulate HPCs after irradiation via proliferation and differentiation. In this study, we also observed the proportion of HSCs and HPCs by flow cytometry.

Irradiation (4 Gy) reduced the proportion of HSCs and HPCs in the bone marrow; however, treatment with 200 mg/kg DTT significantly increased the number of HSCs and HPCs.

Small intestinal crypt cells are most sensitive to the effects of ionizing radiation due to their rapid proliferation rate. Under physiological conditions, intestinal epithelial homeostasis is maintained by proliferative cells in crypts [51]. The recovery of small intestine injury after ionizing radiation has been found to depend on the survival and increase in the number of clonogenic cells in the intestine crypt [52]. High-dose ionizing radiation could induce a decrease in proliferative function among intestinal crypt cells and lead to the increased permeability of the intestinal lining, including the permeability of intestinal bacteria, the potentially bacteremia and the exacerbation of mucosal inflammation [53,54]. Analysis of lethally abdominal irradiated mice injury to DTT treatment, revealed increased proliferative marker expression of Ki-67, which indicated recovery of intestinal crypt cell functions. However, DTT treatment significantly rescued the changes in the basal lamina of the small intestine and the pathological morphology induced by irradiation. Moreover, the biomarker of $Lgr5^+$ stem cells, Olfm4, is a member of the olfactomedin domain-containing proteins. Our results showed that DTT treatment enhanced $Lgr5^+$ stem cell survival and maintained the regeneration capacity of intestinal cells, including $lysozymes^+$ Paneth cells. In general, we concluded that DTT treatment attenuates ABI-induced injury to the small intestine and maintains the regeneration capacity of the small intestine epithelium.

Irradiation induces a variety of DNA injuries, including oxidized base damage, single-strand breaks (SSBs), double-strand breaks (DSBs) and DNA protein crosslinks [55]. DSBs are considered the most lethal lesions induced by irradiation, and one unrepaired DSB can be sufficient to cause cell apoptosis [10,56]. γH2AX as a biomarker for DSBs and was used to assess the effect of new radioprotectors on tissue-specific DNA damage and repair. In our present study, we found that DTT treatment significantly reversed radiation-induced increases in γH2AX expression in the small intestine. The result could be due to fewer double-strand DNA breaks from the antioxidant function and enhanced DNA repair by DTT.

Considering the high toxicity of radiation to the small intestinal system, the underlying mechanisms of radiation-induced intestinal injury are complex. A previous study found that p53 regulates apoptotic responses to a wide range of genotoxic stresses through transcriptional activation of its downstream targets [57]. The pro-apoptotic molecule p53 is essential for a major component of the normal response to irradiation-induced DNA damage, repair, and apoptosis in intestinal mucosal cells [58]. Additionally, p53 is activated and plays roles mainly via irradiation induced single strand or double strand breaks (DSBs) [59]. Activated p53 could stimulate soluble monomeric protein Bax translocate from the cytosol to the mitochondrial outer membrane to feedback and respond to apoptotic signals. Simultaneously, the pro-apoptotic mitochondrial membrane protein Bak was stimulated and expressed. Previous studies reported that the expression of Bax and Bak were upregulated during p53-dependent apoptosis and both induced apoptosis [60,61]. In this study, we found that the expression levels of p53, Bax and Bak were significantly downregulated in DTT treatment. Furthermore, we investigated the influences of irradiation-induced expression of the anti-apoptotic protein Bcl-2, which plays an important role in determining the strength of resistance or sensitivity of cells to various consequences stimulate signals that induce apoptosis [62]. In particular, Bcl-2 are the most important anti-apoptotic members of the Bcl-2 family and can antagonize apoptosis by preventing the signal transmission of pro-apoptotic genes [63,64]. The expression of Bcl-2 was inhibited in irradiated mice; however, DTT treatment was revised. Moreover, caspases involved in apoptosis have been sub-classified by their mechanism of action including initiator caspase (caspase-9) and executioner caspase (caspase-3) [65–67]. The results showed that DTT treatment could ameliorate the sensitivity of intestinal progenitor/stem cells to radiation-induced apoptosis via downregulation of caspase-3 or caspase-9. Therefore, we concluded that p53 is an important target of DTT mediated radioprotection in intestinal stem cells. These findings suggest that suppression of p53 by DTT treatment confers protection from radiation-induced intestinal injury via regulating the intrinsic apoptotic pathway (Fig. 10).

Amifostine (WR-2721) is the only radioprotector that has been approved by the FDA for head and neck cancer. Milas et al. showed that amifostine could protect the small intestine from IR induced injury [68]. Rebecca J. et al. also noted that this drug could inhibit radiation induced hematopoietic progenitor cell apoptosis [69]. However, the effective dose and the minimum toxic dose of amifostine are very close. Severe side-effects of the drug, such as diarrhea, nausea and vomiting limit its extensive use [70]. Furthermore, the daily use of amifostine has been limited due to its hematological and gastrointestinal toxicity [71]. In this study, our data support that DTT can inhibit IR-induced hematopoietic and intestinal injury. The dose (200 mg/kg·day) of DTT used in our study is safely achievable in mice. Doses of up to 500 mg/kg of DTT a day have not been shown the severe side-effects, including diarrhea and vomiting. However, the mice was died when the dose was increased to 600 mg/kg. Unfortunately, our study demonstrates that the toxicity data of DTT is unknown in humans, despite the effort to obtain information from the references. Therefore, we are designing a new type of thiol compounds by optimizing the existing DTT structure to alleviate the toxicity of DTT. We hope that it can help us find radioprotector candidates with higher efficiency via rational drug design and the selection of high-throughput drug screening.

In summary, our study shows that DTT can potentially be used as a radioprotector to effectively mitigate radiation-induced hematopoietic injury and intestinal injury in mice. We also demonstrated that the underlying mechanism of DTT-mediated intestinal radioprotection depends on manipulation of the p53 intrinsic apoptotic pathway. This study provides potential drug design targets for radioprotectors that protect the organism against radiation-induced damage. However, the detailed molecular mechanisms deserve further investigation in the future. In addition, we can explore the links between biological signal pathways, and metabolic networks with drugs to improve the therapeutic index of new radioprotectors.

Authors contributions

Hongqi Tian conceived and designed the research of the paper; Kui Li, Junling Zhang carried out the follow-up experiments with the help from Jian Cao, Xuejiao Li; Kui Li and Junling Zhang analyzed the data and interpreted the results; and Kui Li wrote the manuscript with contributions from Hongqi Tian.

Declaration of Competing Interest

The authors declare that they have no potential conflicts of interest.

Acknowledgments

This work was supported by the CAMS Innovation Fund for Medical Sciences [CIFMS, 2017-I2M-3-019] from the Chinese Academy of Medical Sciences & Peking Union Medical College, and the Tianjin Major Scientific and Technological Projects of New Drug Creation (17ZXXYSY00090).

Appendix A. Supplementary material

Supplementary data to this article can be found online at https://doi.org/10.1016/j.intimp.2019.105913.

References

[1] E.A. McCulloch, J.E. Till, The sensitivity of cells from normal mouse bone marrow

to gamma radiation in vitro and in vivo, Radiat. Res. 16 (1962) 822–832.
[2] J.K. Waselenko, et al., Medical management of the acute radiation syndrome: recommendations of the Strategic National Stockpile Radiation Working Group, Ann. Intern. Med. 140 (2004) 1037–1051.
[3] H. Dorr, V. Meineke, Acute radiation syndrome caused by accidental radiation exposure – therapeutic principles, BMC Med. 9 (2011) 126.
[4] T.B. Elliott, et al., Gastrointestinal acute radiation syndrome in Gottingen minipigs (Sus scrofa domestica), Comp. Med. 64 (2014) 456–463.
[5] C.S. Potten, Radiation, the ideal cytotoxic agent for studying the cell biology of tissues such as the small intestine, Radiat. Res. 161 (2004) 123–136.
[6] J. Wang, et al., A differentiation checkpoint limits hematopoietic stem cell self-renewal in response to DNA damage, Cell 158 (2014) 1444.
[7] N. Dainiak, et al., First global consensus for evidence-based management of the hematopoietic syndrome resulting from exposure to ionizing radiation, Disaster Med. Public Health Prep. 5 (2011) 202–212.
[8] G. Xu, et al., Metformin ameliorates ionizing irradiation-induced long-term hematopoietic stem cell injury in mice, Free Radic. Biol. Med. 87 (2015) 15–25.
[9] Y. Wang, B.A. Schulte, A.C. LaRue, M. Ogawa, D. Zhou, Total body irradiation selectively induces murine hematopoietic stem cell senescence, Blood 107 (2006) 358–366.
[10] L. Shao, Y. Luo, D. Zhou, Hematopoietic stem cell injury induced by ionizing radiation, Antioxid. Redox Signal. 20 (2014) 1447–1462.
[11] D.A. Freshwater, Effects of nuclear weapons on the gastrointestinal system, J. R. Army Med. Corps 150 (2004) 17–21.
[12] T. Ishii, et al., Brief note and evaluation of acute-radiation syndrome and treatment of a Tokai-mura criticality accident patient, J. Radiat. Res. 42 (Suppl) (2001) S167–182.
[13] K.A. Mason, H.R. Withers, W.H. McBride, C.A. Davis, J.B. Smathers, Comparison of the gastrointestinal syndrome after total-body or total-abdominal irradiation, Radiat. Res. 117 (1989) 480–488.
[14] M. Bjerknes, H. Cheng, Clonal analysis of mouse intestinal epithelial progenitors, Gastroenterology 116 (1999) 7–14.
[15] D.G. Kirsch, et al., p53 controls radiation-induced gastrointestinal syndrome in mice independent of apoptosis, Science 327 (2010) 593–596.
[16] N.H. Terry, E.L. Travis, The influence of bone marrow depletion on intestinal radiation damage, Int. J. Radiat. Oncol. Biol. Phys. 17 (1989) 569–573.
[17] E. Jafari, M. Alavi, F. Zal, The evaluation of protective and mitigating effects of vitamin C against side effects induced by radioiodine therapy, Radiat. Environ. Biophys. 57 (2018) 233–240.
[18] M.E. Crowe, C.J. Lieven, A.F. Thompson, N. Sheibani, L.A. Levin, Borane-protected phosphines are redox-active radioprotective agents for endothelial cells, Redox Biol. 6 (2015) 73–79.
[19] M. Werner-Wasik, Future development of amifostine as a radioprotectant, Semin. Oncol. 26 (1999) 129–134.
[20] M.V. Vasin, Comments on the mechanisms of action of radiation protective agents: basis components and their polyvalence, Springerplus 3 (2014) 414.
[21] Y.J. Oh, M.S. Kwak, M.H. Sung, Protection of radiation-induced DNA damage by functional cosmeceutical poly-gamma-glutamate, J. Microbiol. Biotechnol. 28 (2018) 527–533.
[22] A. Ghahghaei, J. Valizadeh, S. Nazari, M. Ravandeh, Chaperone potential of Pulicaria undulata extract in preventing aggregation of stressed proteins, AAPS PharmSciTech 15 (2014) 658–664.
[23] N. Spear, S.D. Aust, The effects of different buffers on the oxidation of DNA by thiols and ferric iron, J. Biochem. Mol. Toxicol. 12 (1998) 125–132.
[24] E.B. Getz, M. Xiao, T. Chakrabarty, R. Cooke, P.R. Selvin, A comparison between the sulfhydryl reductants tris(2-carboxyethyl)phosphine and dithiothreitol for use in protein biochemistry, Anal. Biochem. 273 (1999) 73–80.
[25] S. Zheng, G.L. Newton, G. Gonick, R.C. Fahey, J.F. Ward, Radioprotection of DNA by thiols: relationship between the net charge on a thiol and its ability to protect DNA, Radiat. Res. 114 (1988) 11–27.
[26] K.D. Held, H.A. Harrop, B.D. Michael, Effects of oxygen and sulphydryl-containing compounds on irradiated transforming DNA. II. Glutathione, cysteine and cysteamine, Int. J. Radiat. Biol. Relat. Stud. Phys. Chem. Med. 45 (1984) 615–626.
[27] J.H. Kim, E.J. Lee, J.W. Hyun, S.H. Kim, W. Mar, J.K. Kim, Reduction of radiation-induced chromosome aberration and apoptosis by dithiothreitol, Arch Pharm. Res. 21 (1998) 683–687.
[28] D. Joshi, D.K. Mittal, S. Shukla, A.K. Srivastav, S.K. Srivastav, Methylmercury toxicity: amelioration by selenium and water-soluble chelators as N-acetyl cysteine and dithiothreitol, Cell Biochem. Funct. 32 (2014) 351–360.
[29] M. Omidi, H. Niknahad, A. Mohammadi-Bardbori, Dithiothreitol (DTT) rescues mitochondria from nitrofurantoin-induced mitotoxicity in rat, J. Biochem. Mol. Toxicol. 30 (2016) 588–592.
[30] J.S. Kim, W.S. Jang, S. Lee, Y. Son, S. Park, S.S. Lee, A study of the effect of sequential injection of 5-androstenediol on irradiation-induced myelosuppression in mice, Arch. Pharm. Res. 38 (2015) 1213–1222.
[31] K. Venkateswaran, et al., Mitigation of radiation-induced hematopoietic injury by the polyphenolic acetate 7,8-diacetoxy-4-methylthiocoumarin in mice, Sci. Rep. 6 (2016) 37305.
[32] B.J. Leibowitz, et al., Ionizing irradiation induces acute haematopoietic syndrome and gastrointestinal syndrome independently in mice, Nat. Commun. 5 (2014) 3494.
[33] M. Hauer-Jensen, J. Wang, J.W. Denham, Bowel injury: current and evolving management strategies, Semin. Radiat. Oncol. 13 (2003) 357–371.
[34] J. Wang, et al., Hirudin ameliorates intestinal radiation toxicity in the rat: support for thrombin inhibition as strategy to minimize side-effects after radiation therapy and as countermeasure against radiation exposure, J. Thromb. Haemost. 2 (2004) 2027–2035.
[35] N. Barker, et al., Identification of stem cells in small intestine and colon by marker gene Lgr5, Nature 449 (2007) 1003–1007.
[36] C. Metcalfe, N.M. Kljavin, R. Ybarra, F.J. de Sauvage, Lgr5+ stem cells are indispensable for radiation-induced intestinal regeneration, Cell Stem Cell 14 (2014) 149–159.
[37] K. Cadwell, et al., A key role for autophagy and the autophagy gene Atg16l1 in mouse and human intestinal Paneth cells, Nature 456 (2008) 259–263.
[38] K. Cadwell, et al., Virus-plus-susceptibility gene interaction determines Crohn's disease gene Atg16L1 phenotypes in intestine, Cell 141 (2010) 1135–1145.
[39] A. Kaser, et al., XBP1 links ER stress to intestinal inflammation and confers genetic risk for human inflammatory bowel disease, Cell 134 (2008) 743–756.
[40] M. Hofer, Z. Hoferova, M. Falk, Pharmacological modulation of radiation damage. Does it exist a chance for other substances than hematopoietic growth factors and cytokines? Int. J. Mol. Sci. 18 (2017).
[41] V.K. Singh, T.M. Seed, A review of radiation countermeasures focusing on injury-specific medicinals and regulatory approval status: part I. Radiation sub-syndromes, animal models and FDA-approved countermeasures, Int. J. Radiat Biol. 93 (2017) 851–869.
[42] N. Dainiak, Hematologic consequences of exposure to ionizing radiation, Exp. Hematol. 30 (2002) 513–528.
[43] W. Fendler, et al., Evolutionarily conserved serum microRNAs predict radiation-induced fatality in nonhuman primates, Sci. Transl. Med. (2017;9.).
[44] F.A. Mettler Jr., G.L. Voelz, Major radiation exposure–what to expect and how to respond, N. Engl. J. Med. 346 (2002) 1554–1561.
[45] M. Hatch, E. Cardis, Somatic health effects of Chernobyl: 30 years on, Eur. J. Epidemiol. 32 (2017) 1047–1054.
[46] N.J. Kleiman, F.A. Stewart, E.J. Hall, Modifiers of radiation effects in the eye, Life Sci. Space Res. (Amst.) 15 (2017) 43–54.
[47] T.A. Davis, T.K. Clarke, S.R. Mog, M.R. Landauer, Subcutaneous administration of genistein prior to lethal irradiation supports multilineage, hematopoietic progenitor cell recovery and survival, Int. J. Radiat Biol. 83 (2007) 141–151.
[48] X.L. Xue, et al., Astaxanthin attenuates total body irradiation-induced hematopoietic system injury in mice via inhibition of oxidative stress and apoptosis, Stem Cell Res. Ther. 8 (2017) 7.
[49] J. Farres, et al., Parp-2 is required to maintain hematopoiesis following sublethal gamma-irradiation in mice, Blood 122 (2013) 44–54.
[50] H.L. Chua, et al., Long-term hematopoietic stem cell damage in a murine model of the hematopoietic syndrome of the acute radiation syndrome, Health Phys. 103 (2012) 356–366.
[51] C.S. Potten, H.K. Grant, The relationship between ionizing radiation-induced apoptosis and stem cells in the small and large intestine, Br. J. Cancer 78 (1998) 993–1003.
[52] H. Ishihara, I. Tanaka, H. Yakumaru, M. Tanaka, K. Yokochi, M. Akashi, Pharmaceutical drugs supporting regeneration of small-intestinal mucosa severely damaged by ionizing radiation in mice, J. Radiat. Res. 54 (2013) 1057–1064.
[53] S. Szabo, Z. Sandor, A. Vincze, Z. Gombos, A. Mohiuddin, T. Viravathana, Radiation-induced enterocolitis: basic and applied science, Eur. J. Surg. (1998) 85–89.
[54] H. Ishihara, et al., Acceleration of regeneration of mucosa in small intestine damaged by ionizing radiation using anabolic steroids, Radiat. Res. 175 (2011) 367–374.
[55] J.F. Ward, DNA damage produced by ionizing radiation in mammalian cells: identities, mechanisms of formation, and reparability, Prog. Nucleic Acid Res. Mol. Biol. 35 (1988) 95–125.
[56] B.J. Chen, et al., Growth hormone mitigates against lethal irradiation and enhances hematologic and immune recovery in mice and nonhuman primates, PLoS ONE 5 (2010) e11056.
[57] J. Yu, L. Zhang, The transcriptional targets of p53 in apoptosis control, Biochem. Biophys. Res. Commun. 331 (2005) 851–858.
[58] A.R. Clarke, S. Gledhill, M.L. Hooper, C.C. Bird, A.H. Wyllie, p53 dependence of early apoptotic and proliferative responses within the mouse intestinal epithelium following gamma-irradiation, Oncogene 9 (1994) 1767–1773.
[59] P. Fei, W.S. El-Deiry, P53 and radiation responses, Oncogene 22 (2003) 5774–5783.
[60] J.L. Perfettini, R.T. Kroemer, G. Kroemer, Fatal liaisons of p53 with Bax and Bak, Nat. Cell Biol. 6 (2004) 386–388.
[61] T. Miyashita, J.C. Reed, Tumor suppressor p53 is a direct transcriptional activator of the human bax gene, Cell 80 (1995) 293–299.
[62] S. Zinkel, A. Gross, E. Yang, BCL2 family in DNA damage and cell cycle control, Cell Death Differ. 13 (2006) 1351–1359.
[63] S. Shimizu, et al., Role of Bcl-2 family proteins in a non-apoptotic programmed cell death dependent on autophagy genes, Nat. Cell Biol. 6 (2004) 1221–1228.
[64] A. Morita, et al., Sodium orthovanadate inhibits p53-mediated apoptosis, Cancer Res. 70 (2010) 257–265.
[65] M.C. Maiuri, E. Zalckvar, A. Kimchi, G. Kroemer, Self-eating and self-killing: crosstalk between autophagy and apoptosis, Nat. Rev. Mol. Cell Biol. 8 (2007) 741–752.
[66] D.R. McIlwain, T. Berger, T.W. Mak, Caspase functions in cell death and disease, Cold Spring Harb. Perspect. Biol. 7 (2015).
[67] A. Negroni, S. Cucchiara, L. Stronati, Apoptosis, necrosis, and necroptosis in the gut and intestinal homeostasis, Mediators Inflamm. 2015 (2015) 250762.
[68] L. Milas, N. Hunter, B.O. Reid, H.D. Thames Jr., Protective effects of S-2-(3-aminopropylamino)ethylphosphorothioic acid against radiation damage of normal tissues and a fibrosarcoma in mice, Cancer Res. 42 (1982) 1888–1897.
[69] R.J. Ormsby, et al., Protection from radiation-induced apoptosis by the radioprotector amifostine (WR-2721) is radiation dose dependent, Cell Biol. Toxicol. 30 (2014) 55–66.
[70] M.I. Koukourakis, E. Maltezos, Amifostine administration during radiotherapy for cancer patients with genetic, autoimmune, metabolic and other diseases, Anticancer Drugs 17 (2006) 133–138.
[71] S. Odawara, et al., Polaprezinc protects normal intestinal epithelium against exposure to ionizing radiation in mice, Mol. Clin. Oncol. 5 (2016) 377–381.